# Vortex-lattice transitions in $YNi_2B_2C$: Nature of the 45-degree reorientation

S. J. Levett,[1,2] C. D. Dewhurst,[1] and D. McK. Paul[2]
[1]*Institut Laue Langevin, 6 Rue Jules Horowitz, 38042 Grenoble, France*
[2]*Department of Physics, University of Warwick, Coventry CV4 7AL, United Kingdom*
(Received 30 January 2002; published 8 July 2002)

High-resolution small-angle neutron-scattering (SANS) studies of the vortex lattice (VL) in single-crystal $YNi_2B_2C$ allows us to separate Bragg scattered intensities from the multidomain VL that exists for $B\|c$. A precise determination of the VL unit-cell apex angle, $\beta$, shows that there is a finite transition width associated with the field-driven 45° reorientation of the VL at a field $H_1$. Low- and high-field rhombic VL phases coexist over a finite range of applied field with no continuous distortion of the VL between the two phases. The smooth variation in scattered intensity from each phase through the transition indicates a redistribution of domain populations between the low- and high-field vortex structures. Our data supports the notion of a first-order reorientation phase transition in the VL at $H_1$ in the presence of weak static disorder (vortex pinning).

DOI: 10.1103/PhysRevB.66.014515 PACS number(s): 74.25.Dw, 74.25.Ha, 74.60.−w, 74.70.Dd

Type-II superconductivity is characterized by the ''mixed'' or ''vortex'' state where quantized lines of magnetic flux thread the material and form a vortex lattice (VL). The lowest energy configuration for an array of repulsive magnetic-flux lines is usually a two-dimensional (2D) hexagonal lattice although the energy difference between hexagonal and square packing configurations is small ($\simeq 2\%$).[1,2] Obst[3] demonstrated that a square VL exists in a low-$\kappa$ superconducting Pb-Tl alloy when the magnetic field is orientated along a fourfold symmetry axis due to crystal anisotropy effects. Similar mass anisotropy (i.e., penetration depth) effects have also been observed in Nb.[4,5] In these low-$\kappa$ *s*-wave materials the underlying electronic symmetry can be modified by nonlocal interactions resulting in a fourfold symmetry and ''squaring up'' of the current and field profiles around flux lines. A similar fourfold symmetry can also exist in *p*- or *d*-wave superconductors resulting in a square VL in $Sr_2RuO_4$ over almost the entire phase diagram.[6] In general, mass anisotropy effects alone cannot describe a square VL configuration but must be combined with details of the anisotropic Fermi surface and underlying crystal symmetry.

The discovery[7,8] and successful growth[9] of large, high quality single crystals of the borocarbide superconductors [rare earth (RE)]$Ni_2B_2C$ has encouraged studies of the VL within them. The RE can be occupied by the nonmagnetic (Lu, Y) or magnetic (Er, Tm, Ho, Dy) elements presenting systems that can exhibit both superconductivity and long-range magnetic order at low temperatures.[10,11] The superconducting transition temperature $T_c$ varies from about 15 K for RE = Y and Lu to 6 K for Dy, with the Ginzburg-Landau parameter $\kappa > 5$ and upper critical field $B_{c2}$ as high as 10 T. The normal-state electronic mean free path $l$ is typically an order of magnitude larger than the coherence length [$l \simeq 300$ Å, $\xi_0 \simeq 55$ Å for $YNi_2B_2C$ (Ref. 12) although will be dependent on sample quality], implying that nonlocal interactions are important in describing the properties of these clean superconducting systems. Doping studies, for example, Co into $Lu(Ni_{1-x}Co_x)_2B_2C$, show that increasing dopant concentration reduces the normal-state mean free path, therefore, suppressing nonlocality in the dirty limit.[12–14]

Small-angle neutron scattering (SANS),[15–18] scanning tunneling microscopy,[19] and bitter decoration[20] measurements of the mixed state in the (RE)$Ni_2B_2C$ materials show several field-dependent morphologies and alignments of the VL to particular crystallographic directions. For the nonmagnetic $YNi_2B_2C$ and $LuNi_2B_2C$ compounds a distorted hexagonal or rhombic VL appears to be a generic feature of the VL morphology at low fields with diagonal of the rhombic unit cell aligned with the crystallographic [110] [Fig. 2(b)]. With increasing field the apex angle $\beta$ about the long diagonal axis of the unit cell, decreases steadily from 60° until the VL undergoes a ''sharp'' 45° reorientation with respect to the underlying crystallographic axes (at a field $H_1$ in Refs. 15,21, and 22). Upon further increasing the applied field $\beta$ increases continuously until a square VL is formed ($\beta = 90°$) with side parallel to the crystallographic [110] (at a field $H_2$ in Refs. 15,21, and 22) [Fig. 3(b)]. The high-field square VL appears to be a universal feature of the *H*-*T* phase diagram in clean superconducting (RE)$Ni_2B_2C$ materials driven by nonlocal electrodynamics.[16,17] The physical argument for the field dependence of the VL symmetry for $B\|c$ is quite straight forward: nonlocality introduces a fourfold distortion of supercurrent, which results in a fourfold contribution to the intervortex interaction. At low fields the distance between vortices is relatively large. Since nonlocal effects diminish rapidly at large distances from the core a hexagonal VL is expected. Conversely, as the distance between flux lines becomes comparable with the penetration depth the squarelike current and field profiles surrounding the vortex cores become important and a close-packing argument leads to the minimum energy configuration as square, rather than a hexagonal arrangement of flux lines.

Kogan *et al.*[21,22] and Franz *et al.*[23] have been able to describe the VL structure, orientation and field dependence in the borocarbide materials using nonlocal corrections to the London model. Their theoretical analysis suggests that the 45° reorientation of the VL at $H_1$ should be a thermodynamic first-order phase transition while the transition from a rhombic to square unit cell at a higher field $H_2$ should be second order. More recently, Knigavko *et al.*[24] have reconsidered the nonlocal extension to the London model and the

 

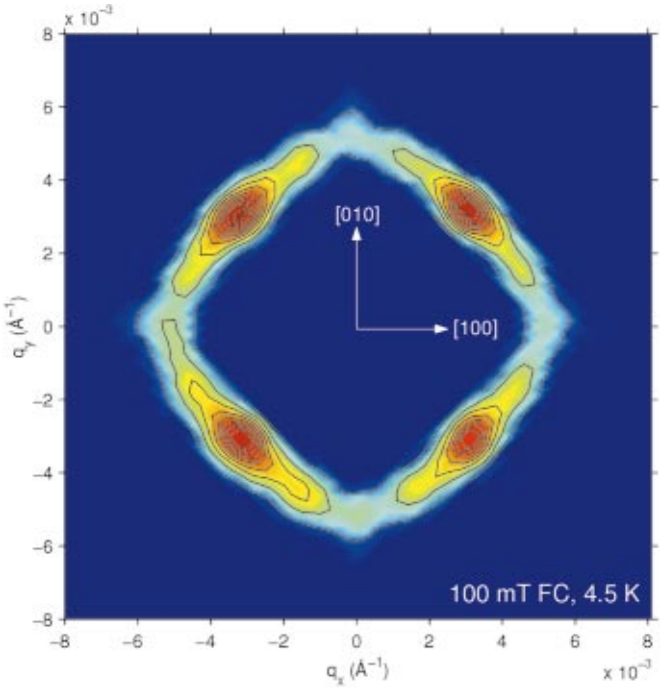


FIG. 1. (Color) SANS diffraction pattern from the VL in $YNi_2B_2C$ prepared by FC to 4.5 K in 100 mT.

expected behavior close to $H_1$. They find that if the unit cell can shear into a more general parallelogram the reorientation at $H_1$ may in fact proceed via two continuous transitions consisting of a gradual rotation of the unit cell accompanied by a small shear deformation with associated orthorhombic to monoclinic and then back to orthorhombic symmetry.

We have performed detailed high-resolution SANS measurements to examine the morphology of the VL in an attempt to elucidate experimentally the nature of the 45° reorientation close to $H_1$. Understanding the role of nonlocality in the VL morphology of the nonmagnetic borocarbide compounds is of key importance if the effects of magnetic ordering on the superconductivity in the mixed state of the magnetic RE ion containing materials are to be quantitatively understood. Furthermore, the nature of any possible first-order phase transitions and the influence of static (pinning) and dynamic (thermal) disordering effects is of topical and fundamental scientific interest with respect to the first-order VL melting transition in high-temperature superconducting materials.[25]

SANS measurements were carried out using the D22 diffractometer at the Institut Laue Langevin, Grenoble, France. The instrument was configured in a high-resolution mode using a mean incident neutron wavelength of 10 Å with 10% wavelength spread and collimation defined by a 30-mm-diameter circular aperture and 5-mm sample aperture separated by a collimation length of 17.06 m. The diffracted intensity was imaged using a $128\times128$ (7.5 $mm^2$) pixel area detector 17 m from the sample. To maximize the intensity for any particular diffraction spot the sample and electromagnet could be tilted together about a horizontal or vertical axis to satisfy the Bragg condition for that spot. Background measurements, taken with the sample in the normal state ($T > T_c$), have been subtracted from each pattern prior to analysis. The $YNi_2B_2C$ single crystal used for these measurements was grown using a high-temperature flux method with isotopic $^{11}B$ to reduce neutron absorption, as described elsewhere.[9]

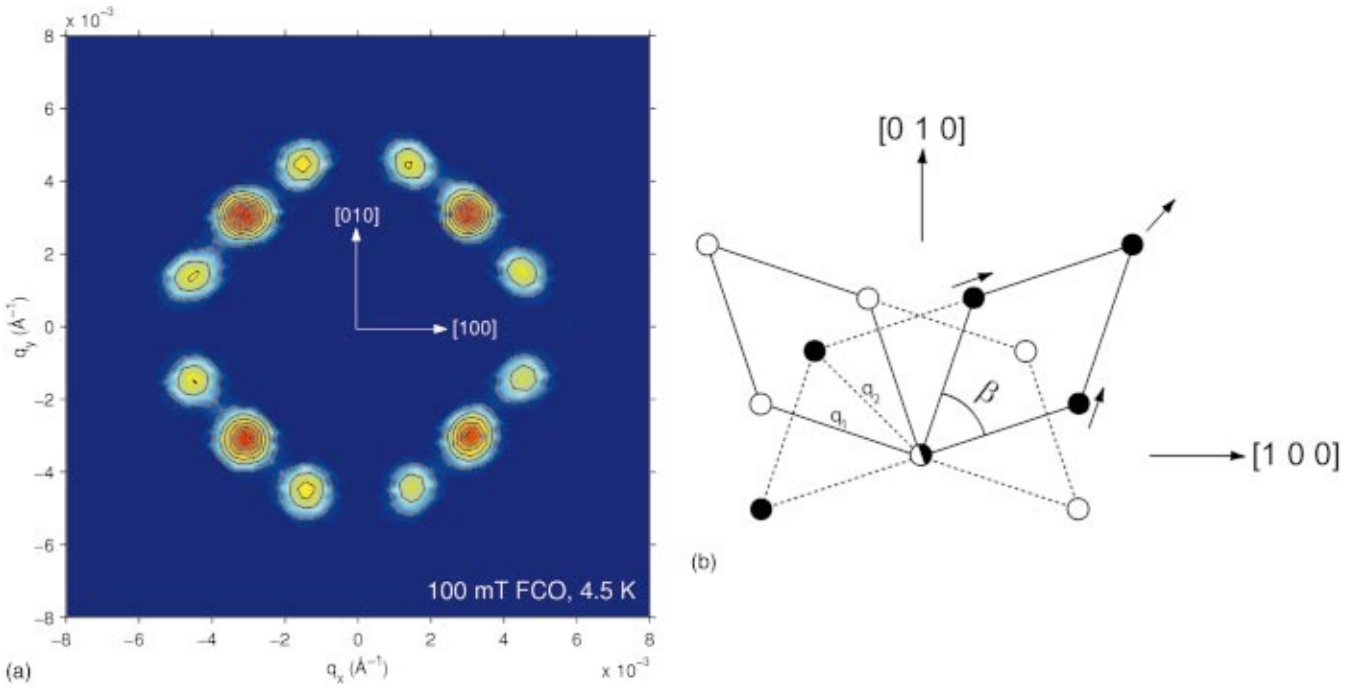


FIG. 2. (Color) (a) SANS diffraction pattern from the VL in $YNi_2B_2C$ at 4.5 K, prepared using the FCO preparation technique in 100 mT. The VL is the same as that in Fig. 1 but after application of the small damped oscillating field. (b) Schematic of the two-domain low-field phase with orientation of the diagonals of the rhombic unit cells along the [110] and $[\bar{1}10]$ directions.

A VL can be ''grown'' within the superconducting crystal by various combinations of field and temperature histories as the sample enters the superconducting state from above either $T_c$ or $B_{c2}$. In principle, cooling the crystal through $T_c$ in the chosen applied magnetic field [field cooling (FC)] should generate a magnetic-field distribution close to the equilibrium magnetization or VL arrangement.[26] On the other hand, vortex pinning often disorders and introduces mosaic in the FC VL structure due to competition between Meissner expulsion of flux and pinning as the sample is cooled below $T_c$. Other field-temperature profiles attempting to prepare a nominally ''equilibrium'' VL all suffer from competition between Meissner expulsion and pinning effects. For example zero-field cooling (ZFC) to the destination temperature followed by application of the desired field results in a nonequilibrium VL with the sample in a Bean-like critical state.[27] A similar result is expected by cooling in an applied field much higher than the desired value, possibly even higher than $B_{c2}$, before lowering the field to the chosen value [high-field cooling (HFC)]. In a superconductor with significant pinning, the ZFC and HFC process effectively result in a sample magnetization of approximately opposite signs on either side of the hysteretic magnetization curve. The FC procedure is generally considered to result in a VL state closest to its equilibrium.[26]

Figure 1 shows a diffraction image from the VL following field cooling in 100 mT to 4.5 K. The VL resulting from the FC procedure is clearly rather disordered. At low fields (below about 100 mT) the VL in $YNi_2B_2C$ should in fact be almost hexagonal, consisting of two equivalent, orthogonal domains when the field is aligned along the $c$ axis of the tetragonal crystal.[15] Closer inspection of Fig. 1, however, shows that scattered intensity lies predominantly on, and extended azimuthally, about either side of four principal Bragg reflections. The azimuthally distributed scattered intensity does not lie on a circle, i.e., constant scattering vector $|\mathbf{q}|$, but lies on a ''squared-off'' ring of intensity. We have found the partially disordered FC VL to be a common observation in our SANS studies of borocarbide materials despite the fact that bulk pinning in these materials is thought to be rather weak with a *bulk* critical current density, $J_c$, of the order $10^3$ A cm$^{-2}$.[28–30]

In an attempt to improve the spatial order of the vortex lines and achieve a more equilibrium VL arrangement we have used an oscillating field technique to postanneal the FC VL and better resolve scattered intensities from individual Bragg reflections. After FC to the desired temperature the applied field was sinusoidally oscillated with exponentially damped initial amplitude of 10% of the FC value. The field-cooled and oscillating (FCO) technique is analogous to ''shaking'' the VL assisting thermal activation in an attempt to achieve a vortex arrangement closer to the true equilibrium and has been applied by other workers elsewhere.[31–33] An image of the FCO prepared VL (100 mT, 4.5 K) is shown in Fig. 2(a) and is in fact the *same* VL as that shown in Fig. 1 measured after field oscillation. The improvement in orientational order is quite remarkable. Figure 2(a) shows 12 Bragg peaks from two domains of rhombic VL. The mean change in intervortex spacing at peak amplitude during oscillation is around 5% and therefore should not introduce significant changes in the bulk vortex behavior. Oscillation simply shakes the VL to promote ordering by allowing vortices to move away from randomly distributed pinning sites. Using the Bean critical state model, a value for the *bulk* critical current density of $10^3$ A cm$^{-2}$ (Ref. 30) and our crystal dimensions, a quick calculation[34] shows that an amplitude of a few tens of milli Tesla (i.e., around 10% of the main field) should be sufficient to fully penetrate the crystal. The remaining data presented in this paper has been measured using the FCO VL preparation procedure with 10% amplitude. We believe the field oscillation procedure results in a VL distribution closer to the equilibrium, especially when pinning and static disordering of the VL becomes significant for fields below about 100 mT in $YNi_2B_2C$.[30]

Figure 2(a) shows the SANS diffraction pattern from $YNi_2B_2C$ at low fields, i.e., $H<H_1$. The positions of the twelve Bragg peaks do not lie on a circle of constant $|\mathbf{q}|$, as would be expected from a VL with hexagonal symmetry. Instead the diffraction pattern consists of four intense Bragg reflections with two weaker peaks on either side. The diffraction pattern corresponds to two domains of rhombic VL with opening angle $\beta$ smaller than 60°, as shown schematically in Fig. 2(b). By fitting 2D Gaussian functions to the multidetector data for each Bragg reflection we are able to accurately determine $\beta$. For the data presented in Fig. 2(a) at 100 mT and 4.5 K, $\beta \simeq 54°$. To our knowledge, these data represent the first successful resolution of Bragg scattering from the two domain low-field VL state for $B \| c$ using SANS. Due to the azimuthal broadening that occurs in the FC lattice (Fig. 1), previous SANS experiments were mostly carried out with **B** inclined to **c** in order to break the fourfold symmetry and force a single VL domain.[15] In Fig. 2(a) we have been able to overcome the increasing disordering effects of pinning at low fields by using the FCO VL preparation technique described above.

It is interesting to note that due to the rhombic geometry of the unit cell, the positions of the twelve first-order Bragg reflections appear at different $|\mathbf{q}|$ values, $q_1$ and $q_2$ as depicted schematically in Fig. 2(b). For the data presented in Fig. 2(a) with $\beta \sim 54°$, $q_1$ and $q_2$ differ by around 9%. The integrated intensity $I_{hk}$ of an $(h,k)$ diffraction spot depends on the square of the form factor $F_{hk}$ and the magnitude of the scattering vector $q_{hk}$ via:[35]

$$I_{hk} = 2\pi V \phi \left(\frac{\gamma}{4}\right)^2 \frac{\lambda_n^2}{\Phi_0^2 q_{hk}} |F_{hk}|^2, \tag{1}$$

where $V$ is the illuminated sample volume, or domain volume contributing to the Bragg reflection, $\phi$ is the neutron flux, $\lambda_n$ is the neutron wavelength, $\gamma$ is the neutron magnetic moment and $\Phi_0$ is the flux quantum. For high-$\kappa$ materials, the approximate (London) form for $F_{hk}$ is

$$F_{hk} = \frac{B}{1 + q_{hk}^2 \lambda^2} \tag{2}$$

ignoring contributions from the finite-sized vortex core. Since $q_{hk}^2 \lambda^2 \gg 1$ in this case the intensity of the Bragg reflec-

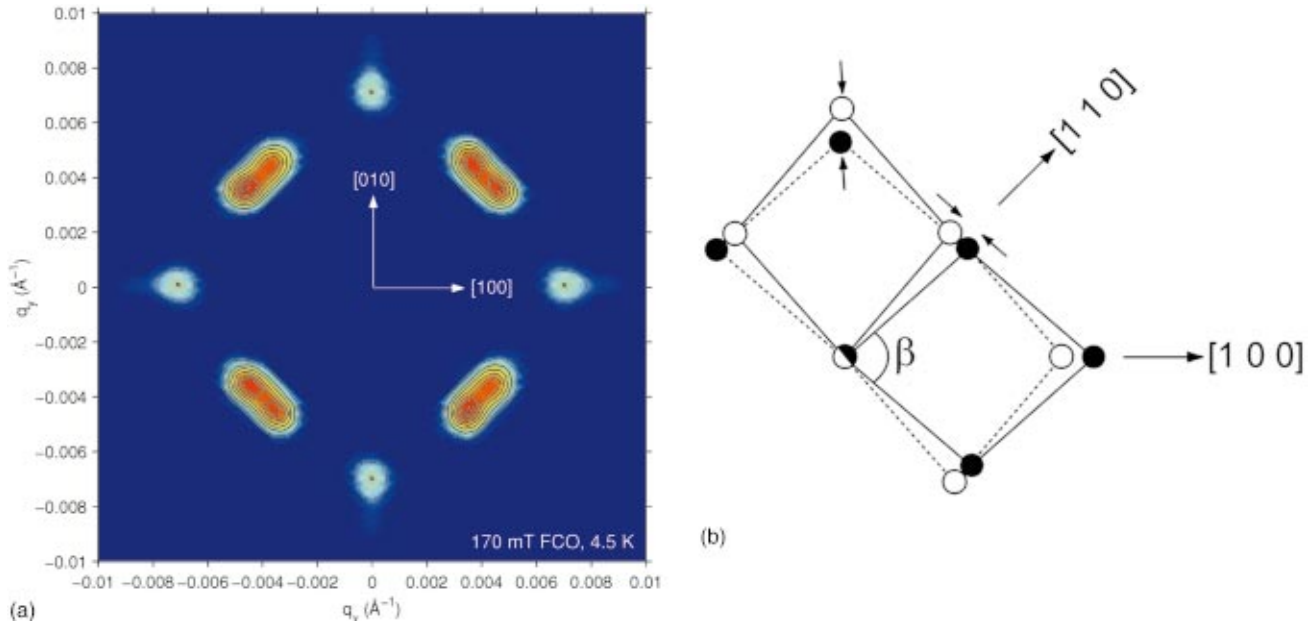


FIG. 3. (Color) (a) SANS diffraction pattern from the VL in $YNi_2B_2C$ at 4.5 K, FCO in 170 mT (image symmetrized about one fully measured quadrant). (b) Schematic of the two-domain high-field phase with orientation of the diagonals of the rhombic unit cells along the [010] and [100] directions.

tions varies approximately as $1/q_{hk}^5$. Using the measured values of $q_1$ and $q_2$ as 4.72 $Å^{-1}$ and 4.32 $Å^{-1}$ the ratio of intensities between the two spots should be around 1.6, close to the value of 1.8 we find for the data presented in Fig. 2(a). With increasing field, $\beta$ decreases continuously as the rhombic unit cell distorts along the direction of its diagonal until reorientation at $H_1$. The data presented in Fig. 2(a) is representative of that measured at low fields below the reorientation field for this crystal ($H_1 \simeq 140$ mT).

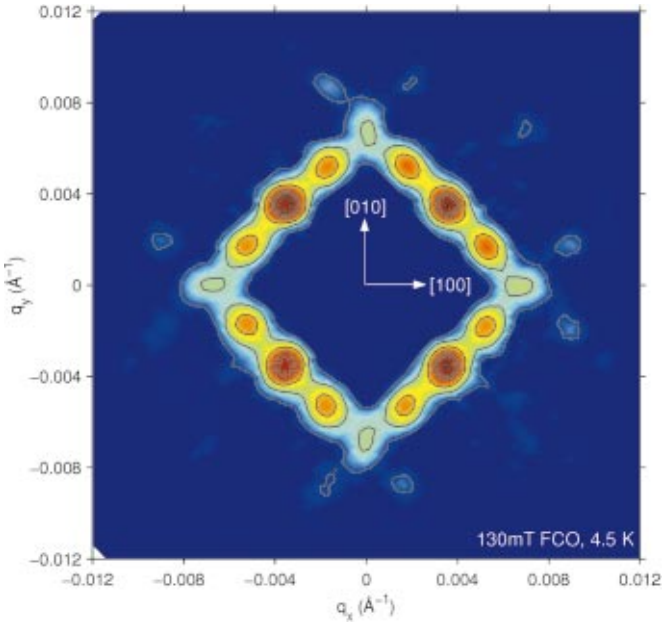


FIG. 4. (Color) SANS diffraction pattern from the VL in $YNi_2B_2C$ at 4.5 K, FCO in 130 mT, illustrating a coexistence of both the low- and high-field rhombic VL phases near $H_1$.

Figure 3(a) shows the VL at 170 mT (i.e., above $H_1$) where the rhombic VL has reorientated by 45° and $\beta$ has abruptly switched to a value greater than 60°. For the data presented in Fig. 3(a) at 170 mT $\beta \simeq 82°$ with rhombic unit-cell diagonals now oriented along the [100] and [010] crystallographic directions [Fig. 3(b)]. The corresponding SANS diffraction pattern possesses eight first-order Bragg peaks, present in pairs. Each pair of spots is split azimuthally while the visible higher-order (1,1) reflections are extended in the radial direction as expected, although not optimized in intensity (''rocked on'') in Fig. 3(a). A schematic representation of the two-domain high-field rhombic lattice structure is presented in Fig. 3(b). With further increasing the applied field, $\beta$ increases continuously until $\beta = 90°$ with a single square VL domain.[15]

We now turn our attention to the transition region close to $H_1$. Figure 4 shows the diffraction image from the VL measured at a field of 130 mT. The diffraction pattern shown is rather complex suggesting that the VL at this field consists of several domains of different structure and orientation. By comparison with Fig. 2, evidence of the low-field phase is clearly apparent. At the same time the four most intense Bragg peaks begin to broaden coincident with the appearance of scattered intensity at the (1,1) position associated with the high-field distorted rhombic VL phase (top bottom and left right of image). The data presented in Fig. 4 strongly suggests a coexistence of both the low- and high-field rhombic VL phases depicted individually in Figs. 2 and 3. The positions of much weaker higher-order reflections can only be explained if both phases are simultaneously present. The two phases appear to coexist over a narrow field window about $H_1$, between 110 mT and 170 mT.

Figure 5 shows $\beta$ over a wide field range from the low-field rhombic, through the high-field rhombic phase until the

lattice becomes square. High-resolution SANS and our field oscillation VL preparation techniques have allowed us to determine $\beta$ accurately through $H_1$ where we apparently see a coexistence of both low- and high-field phases (by multiple 2D Gaussian fits to the multidetector data). The VL structure does not appear to smoothly deform through $H_1$ synonymous with a continuous reorientation transition. Instead, $\beta$ takes two well-defined values corresponding to the VL phases below and above $H_1$. The inset to Fig. 5 shows the scattered intensity associated with the low- and high-field phases as a function of field through the coexistence regime. Here, intensity data is shown for the low-field only first order peaks (at $q_1$ in Fig. 2) and the (1,1) diffraction peaks associated with only the high-field rhombus (Fig. 3). In each case the intensity has been normalized by the respective $q^5$ and $B^2$ terms, in order to remove the $q$ and $B$ dependence of scattered intensity from the VL [see Eqs. (1) and (2)]. The resulting quantity is then directly proportional to the population of each type of domain present. The inset to Fig. 5 provides convincing evidence for coexistence of two VL phases and a crossover in the relative intensities associated with the two phases as low- and high-field domain populations vary with increasing field.

The broadened nature of the suggested first-order transition at $H_1$ is due to a weak static disordering (pinning) of the VL. An entirely analogous behavior is seen in the nonuniform melting of the VL in the high-temperature superconducting $Bi_2Sr_2CaCu_2O_{8+\delta}$ compound in single crystals with finite pinning or crystallographic disorder features.[25] Indeed, general arguments[36] suggest that first-order transitions become less sharp in the presence of weak disorder while extreme disorder can transform them into second-order transitions. The effect of disorder in the present case is to create a local variation in transition field $H_1$ (or VL melting temperature in Ref. 25). As pointed out by Franz *et al.*,[23] the free-energy difference between the two phases is very small in the region close to $H_1$ and it is thus likely that real systems should remain in a metastable state and experiment would detect only a smooth crossover from lattices with $\beta<60°$ to one with $\beta>60°$. Both the reorientation of the VL described here and melting of the VL offer[25] excellent examples for the study of first-order transitions in vortex matter in the presence of weak static disorder.

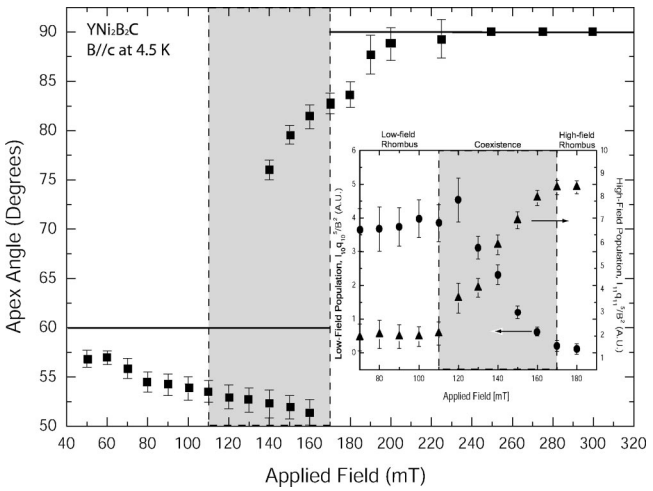


FIG. 5. Apex angle $\beta$ of the VL unit cell vs field at 4.5 K. The shaded region represents the finite region of coexistence of the two mutually rotated VL phases. Inset: Relative populations of the low- and high-field phases about $H_1$.

In summary, we have used high-resolution SANS to determine the nature of the 45° reorientation of the vortex lattice in $YNi_2B_2C$, driven by nonlocal interactions when $B\|c$. Our data illustrates the coexistence of both low- and high-field VL phases over a narrow field range (60 mT) with the VL taking discrete values for the apex angle, $\beta$, at either side of the transition. Our data supports the notion of a first-order phase transition in the vortex lattice at $H_1$ and, within the resolution of our measurement, we find no evidence for a smooth rotation of the unit cell between the two phases. Broadening of the macroscopic transition width and coexistence of low- and high-field rotated VL phases is consistent with the behavior expected from a first-order transition in the presence of weak static disorder (vortex pinning).

[1] W. H. Kleiner, L. M. Roth, and S. H. Autler, Phys. Rev. **133**, 1226 (1964); A. A. Abrikosov, Sov. Phys. JETP **5**, 1174 (1957).
[2] L. Kramer, Phys. Lett. **23**, 619 (1966).
[3] B. Obst, Phys. Lett. **28A**, 662 (1969).
[4] D. Cribier, Y. Simon, and P. Thorel, Phys. Rev. Lett. **28**, 1370 (1972).
[5] D. K. Christen, H. R. Kerchner, S. T. Sekula, and P. Thorel, Phys. Rev. B **21**, 102 (1980).
[6] T. M. Riseman, P. G. Kealey, E. M. Forgan, A. P. Mackenzie, L. M. Galvin, A. W. Tyler, S. L. Lee, C. Ager, D. McK. Paul, C. M. Aegerter, R. Cubitt, Z. Q. Mao, T. Akima, and Y. Maeno, Nature (London) **396**, 242 (1998).
[7] R. Nagarajan, C. Mazumdar, Z. Hossain, S. K. Dhar, K. V. Gopalakrishnan, L. C. Gupta, C. Godart, B. D. Padalia, and R. Vijayaraghavan, Phys. Rev. Lett. **72**, 274 (1994).
[8] R. J. Cava, H. Takagi, H. W. Zandbergen, J. J. Krajewski, W. F. Peck, Jr., T. Siegrist, B. Batlogg, R. B. van Dover, R. J. Felder, K. Mizuhashi, J. O. Lee, H. Eisaki, and S. Uchida, Nature (London) **367**, 252 (1994).
[9] B. K. Cho, P. C. Canfield, L. L. Miller, D. C. Johnston, W. P. Beyermann, and A. Yatskar, Phys. Rev. B **52**, 3684 (1995).
[10] J. W. Lynn, S. Skanthakumar, Q. Huang, S. K. Sinha, Z. Hossain, L. C. Gupta, R. Nagarajan, and C. Godart, Phys. Rev. B **55**, 6584 (1997).
[11] P. C. Canfield, P. L. Gammel, and D. J. Bishop, Phys. Today **51** (10), 40 (1998).
[12] S. V. Shulga, S.-L. Drechsler, G. Fuchs, K.-H. Muller, K. Winzer, H. Heinecke, and K. Krug, Phys. Rev. Lett. **80**, 1730 (1998).
[13] K. O. Cheon, I. R. Fisher, V. G. Kogan, P. C. Canfield, P. Miranovič, and P. L. Gammel, Phys. Rev. B **58**, 6463 (1998).
[14] P. L. Gammel, D. J. Bishop, M. R. Eskildsen, K. Mortensen, N. H. Andersen, I. R. Fisher, K. O. Cheon, P. C. Canfield, and V. G.

Kogan, Phys. Rev. Lett. **82**, 4082 (1999).
[15] D. McK. Paul, C. V. Tomy, C. M. Aegerter, R. Cubitt, S. H. Lloyd, E. M. Forgan, S. L. Lee, and M. Yethiraj, Phys. Rev. Lett. **80**, 1517 (1998).
[16] M. Yethiraj, D. McK. Paul, and E. M. Forgan, Phys. Rev. Lett. **78**, 4849 (1997).
[17] M. Yethiraj, D. McK. Paul, C. V. Tomy, and J. R. Thompson, Phys. Rev. B **58**, R14 767 (1998).
[18] M. R. Eskildsen, K. Harada, P. L. Gammel, A. B. Abrahamsen, N. H. Andersen, G. Ernst, A. P. Ramirez, D. J. Bishop, K. Mortensen, D. G. Naugle, K. D. D. Rathnayakas, and P. C. Canfield, Nature (London) **393**, 242 (1998).
[19] Y. De Wilde, M. Iavarone, U. Welp, V. Metlushko, A. E. Koshelev, I. Aranson, and G. W. Crabtree, Phys. Rev. Lett. **78**, 4273 (1997).
[20] L. Ya. Vinnikov, T. L. Barkov, P. C. Canfield, S. L. Bud'ko, J. E. Ostenson, F. D. Laabs, and V. G. Kogan, Phys. Rev. B **64**, 220508 (2001).
[21] V. G. Kogan, M. Bullock, B. Harmon, P. Miranovic, Lj. Dobrosavljevic-Grujic, P. L. Gammel, and D. J. Bishop, Phys. Rev. B **55**, R8693 (1997).
[22] V. G. Kogan, P. Miranovic, and D. McK. Paul, *The Superconducting State in Magnetic Fields*, edited by Sa de Melo (World Scientific, Singapore, 1998).
[23] M. Franz, I. Affleck, and M. H. S. Amin, Phys. Rev. Lett. **79**, 1555 (1997).
[24] A. Knigavko, V. G. Kogan, B. Rosensten, and T.-J. Yang, Phys. Rev. B **62**, 111 (2000).
[25] A. Soibel, E. Zeldov, M. Rappaport, Y. Myasoedov, T. Tamegai, S. Ooi, M. Konczykowski, and V. B. Geshkenbein, Nature (London) **406**, 282 (2000).
[26] U. Yaron, P. L. Gammel, D. A. Huse, R. N. Kleiman, C. S. Oglesby, E. Bucher, B. Batlogg, and D. J. Bishop, Phys. Rev. Lett. **73**, 2748 (1994).
[27] C. P. Bean, Rev. Mod. Phys. **36**, 31 (1964).
[28] C. D. Dewhurst, R. A. Doyle, E. Zeldov, and D. McK. Paul, Phys. Rev. Lett. **82**, 827 (1999).
[29] C. D. Dewhurst, S. S. James, R. A. Doyle, Y. Paltiel, H. Shtrikman, E. Zeldov, and D. McK. Paul, Phys. Rev. B **63**, 060501(R) (2000).
[30] S. S. James, C. D. Dewhurst, R. A. Doyle, D. McK. Paul, Y. Paltiel, E. Zeldov, and A. M. Campbell, Physica C **332**, 173 (2000).
[31] M. Willemin, A. Schilling, H. Keller, C. Rossel, J. Hofer, U. Welp, W. K. Kwok, R. J. Olsson, and G. W. Crabtree, Phys. Rev. Lett. **81**, 4236 (1998).
[32] A. Huxley, P. Rodiere, D. McK. Paul, N. van Dijk, R. Cubitt, and J. Flouquet, Nature (London) **406**, 160 (2000).
[33] N. Avraham, B. Khaykovich, Y. Myasoedov, M. Rappaport, H. Shtrikman, D. E. Feldman, T. Tamegai, P. H. Kes, M. Li, M. Konczykowski, K. van der Beek, and E. Zeldov, Nature (London) **411**, 451 (2001).
[34] For a simple Bean-like critical state simplified to 1D, $\Delta x \simeq \Delta B/\mu_0 J_c$, where $\Delta x$ is the maximum depth to which the oscillating field profile penetrates at peak amplitude $\Delta B$ with critical current $J_c$. Using $\Delta B \simeq 10$ mT and $J_c \simeq 10^3$ A cm$^{-2}$ gives $\Delta x \simeq 1$ mm, which is of the order of the crystal dimension.
[35] D. K. Christen, F. Tasset, S. Spooner, and H. A. Mook, Phys. Rev. B **15**, 4506 (1977).
[36] Y. Imry and M. Wortis, Phys. Rev. B **19**, 3580 (1979).